Shape-Independent Limits to Near-Field Radiative Heat Transfer

Owen D. Miller, Steven G. Johnson, and Alejandro W. Rodriguez

Shape-independent limits to near-field spectral radiative heat transfer

Owen D. Miller,[1] Steven G. Johnson,[1] and Alejandro W. Rodriguez[2]

[1]*Department of Mathematics, Massachusetts Institute of Technology, Cambridge, MA 02139*
[2]*Department of Electrical Engineering, Princeton University, Princeton, NJ 08544*

We derive shape-independent limits to the spectral radiative heat-transfer rate between two closely spaced bodies, generalizing the concept of a black body to the case of near-field energy transfer. Through conservation of energy and reciprocity, we show that each body of susceptibility χ can emit and absorb radiation at enhanced rates bounded by $|\chi|^2/\operatorname{Im}\chi$, optimally mediated by near-field photon transfer proportional to $1/d^2$ across a separation distance d. Dipole–dipole and dipole–plate structures approach restricted versions of the limit, but common large-area structures do not exhibit the material enhancement factor and thus fall short of the general limit. By contrast, we find that particle arrays interacting in an idealized Born approximation (i.e., neglecting multiple scattering) exhibit both enhancement factors, suggesting the possibility of orders-of-magnitude improvement beyond previous designs and the potential for radiative heat transfer to be comparable to conductive heat transfer through air at room temperature, and significantly greater at higher temperatures.

Heat exchange mediated by photons, or radiative heat transfer, can be dramatically modified for bodies separated by small gaps [1–7]. We exploit energy-conservation and reciprocity principles to derive fundamental limits to the near-field spectral heat flux between closely spaced bodies of arbitrary shape, given only their material susceptibilities $\chi(\omega)$ and their separation distance d. Our approach enables us to define optimal absorbers and emitters in the near field, which contrast sharply with far-field black bodies: their response is bounded by the amplitude of their volume polarization currents, rather than their surface absorptivities, and maximum energy transfer requires coordinated design of the two bodies (whereas the far-field limit derives from the properties of a single black body). These distinguishing characteristics lead to two possible enhancements relative to black-body emission: a material enhancement factor $|\chi(\omega)|^2/\operatorname{Im}\chi(\omega)$ that represents the maximum absorber and emitter polarization currents, and a near-field enhancement factor $1/d^2$ that represents maximum interaction between currents in free space. We show that restricted versions of our limits can be approached for sphere–sphere and sphere–plate configurations. For two extended structures, however, common planar geometries—including bulk metals [8–17], metamaterials [18–24], and thin films [25–31]—exhibit flux rates orders of magnitude short of the limits because they do not satisfy the optimal-absorber condition. Instead, we find that idealized plasmonic-particle arrays, interacting within a Born approximation with negligible multiple scattering, approach the limits at selected frequencies, and that the possibility of reaching the limits, even over a narrow bandwidth (a desirable feature for thermophotovoltaics [7, 32–35]), would represent an orders-of-magnitude improvement over current designs.

A ray-optical black body absorbs every photon incident upon its surface, which by reciprocity (Kirchoff's Law) yields its emissivity and the black-body limit to thermal radiation [36]. At wavelength and subwavelength scales, nanostructures can exhibit optical cross-sections much larger than their physical cross-sections [37], making it difficult even to define quantities like emissivity. A further difficulty in the near field is the presence of evanescent waves, which can in-

crease transmitted power but only through interference with reflected waves [38]. Although the possibility of enhancement beyond the blackbody limit was realized by Rytov, Polder, and others in the 1950s [1, 2], efforts to find underlying limits have been restricted to planar structures with translation symmetry (including metamaterials), without consideration of material loss [10, 15–17, 21, 30]. Spherical-harmonic [39, 40] and Green's-function [41] limits are difficult to apply in the near field where a large but unknown number of spherical harmonics can be excited by general shapes [42].

Without reference to particular structures or symmetries, assuming only linear electromagnetism, we translate the reciprocity principle to the near field by applying it to polarization currents within the bodies. Dipoles in vacuum exchange energy at a rate limited by the energy density of an outgoing free-space wave [43]. As we show below, the maximum energy transfer between material bodies occurs when the currents within the bodies couple individually at the dipole–dipole limit, amplified by material enhancement factors. These conditions allow for much greater heat transfer than has previously been shown possible.

Radiative heat exchange is depicted schematically in Fig. 1(a): fluctuating currents arise in body 1 at temperature T_1, and transfer energy to body 2 at a rate of [4]

$$H_{1\to 2} = \int_0^\infty \Phi(\omega)\left[\Theta(\omega, T_1) - \Theta(\omega, T_2)\right] \mathrm{d}\omega, \quad (1)$$

where $\Phi(\omega)$ is a temperature-independent energy flux and Θ is the Planck spectrum. $\Phi(\omega)$ is the designable quantity of interest, to be tailored as a function of frequency depending on the application and available materials.

Limits—The spectral heat flux $\Phi(\omega)$ is the power absorbed in body 2 from fluctuating sources in body 1 (or vice versa). In recent work [42] we have bounded the scattering properties of any dissipative medium excited by a known, externally generated incident field. The bounds arise from the functional dependencies of power expressions with respect to induced currents: absorption is a quadratic functional, whereas extinction (absorption+scattering), given by the optical theorem [44–47], is only a linear functional. Energy conservation requires that
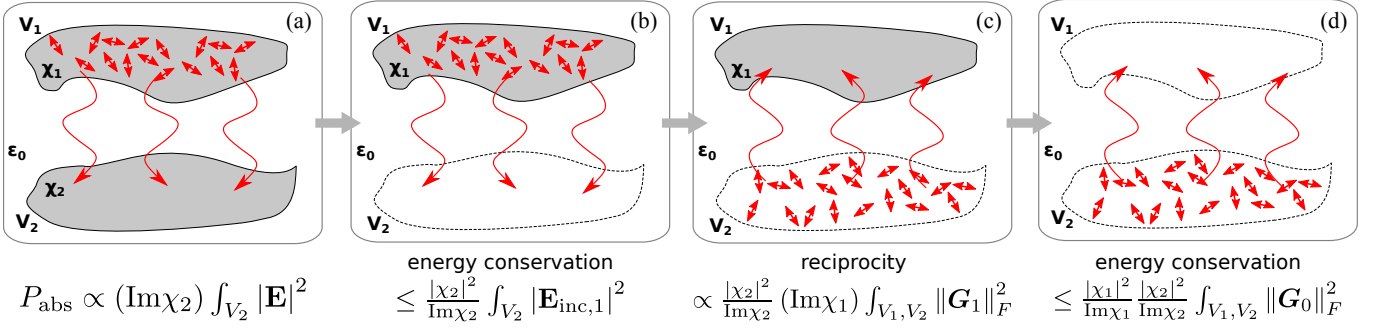
$$P_{\text{abs}} \propto (\text{Im}\chi_2) \int_{V_2} |\mathbf{E}|^2$$

energy conservation
$$\leq \frac{|\chi_2|^2}{\text{Im}\chi_2} \int_{V_2} |\mathbf{E}_{\text{inc},1}|^2$$

reciprocity
$$\propto \frac{|\chi_2|^2}{\text{Im}\chi_2} (\text{Im}\chi_1) \int_{V_1,V_2} \|\mathbf{G}_1\|_F^2$$

energy conservation
$$\leq \frac{|\chi_1|^2}{\text{Im}\chi_1} \frac{|\chi_2|^2}{\text{Im}\chi_2} \int_{V_1,V_2} \|\mathbf{G}_0\|_F^2$$

FIG. 1. (a) Radiative heat transfer: Fluctuating currents in an emitter (body 1, susceptibility χ_1) generate a field $\mathbf{E}_{\text{inc},1}$ and transfer energy to an absorber (body 2, susceptibility χ_2) at a rate $P_{\text{abs},2}$. (b) Energy conservation bounds $P_{\text{abs},2}$ in terms of $\mathbf{E}_{\text{inc},1}$, and a resonant enhancement factor $|\chi_2|^2 / \text{Im}\,\chi_2$. (c) The sources and "receivers" can be exchanged by reciprocity, whereupon (d) absorption in body 1 is bounded, yielding a spectral-flux limit determined by χ_1, χ_2, and the free-space GF $\mathbf{G}_0$. For near-field transfer the GF integral is $\sim 1/d^2$, for separation d.

extinction be greater than absorption, which imposes a bound on the magnitude of the excited currents. Radiative heat transfer, however, involves sources *within* one of the scatterers, preventing a simple optical theorem.

To circumvent this issue we reframe the scattering problem (without approximation). We define the "incident" field to be the unknown field emanating from body 1, and the "scattered" field to arise only with the introduction of body 2. For a Green's function (GF) $\mathbf{G}^1$ that is the field of dipole in the presence of body 1, the fields are given by a standard integral-equation separation [48], $\mathbf{E}_{\text{inc},1} = (i/\varepsilon_0\omega) \int_{V_1} \mathbf{G}_1 \mathbf{J}$ and $\mathbf{E}_{\text{scat},1} = \int_{V_2} \mathbf{G}_1 \mathbf{P}$, where $\mathbf{J}$ are the stochastic source currents in body 1, $\mathbf{P}$ is the polarization field induced in body 2, and ε_0 is the vacuum permittivity. This decomposition permits an optimal theorem with respect to body 2, such that its extinction is proportional to $\text{Im} \int_{V_2} \overline{\mathbf{E}_{\text{inc},1}} \cdot \mathbf{P}$ (its absorption [44] is proportional to $\int_{V_2} |\mathbf{P}|^2$). The energy-conservation arguments from above imply that absorption in body 2 is bounded,

$$P_{\text{abs},2} \leq \frac{\varepsilon_0 \omega}{2} \frac{|\chi_2(\omega)|^2}{\text{Im}\,\chi_2(\omega)} \int_{V_2} |\mathbf{E}_{\text{inc},1}(\mathbf{x}_2)|^2, \quad (2)$$

which is formally derived by variational calculus [42]. To achieve this limit, the optimal polarization field must be proportional to the incident field, $\mathbf{P} \sim \mathbf{E}_{\text{inc},1}$, to maximize the extinction overlap integral. In the near field, where source fields rapidly decay, negative-permittivity metals that support surface-plasmon modes can achieve this condition, as we will demonstrate.

The limit in Eq. (2) reduces the optimal-flux problem to a question of how large the emitted field $\mathbf{E}_{\text{inc},1}$ can be in V_2. Inserting $\mathbf{E}_{\text{inc},1}$ into Eq. (2) yields an integral of the stochastic currents, which is determined by the fluctuation-dissipation theorem [4], $\left\langle J_j(\mathbf{x},\omega), \overline{J_k(\mathbf{x}',\omega)} \right\rangle = 4\varepsilon_0 \omega \Theta(\omega, T_1) \, \text{Im}\,[\chi(\omega)] \delta_{jk} \delta(\mathbf{x} - \mathbf{x}')/\pi$, such that the ensemble-averaged emitted field at $\mathbf{x}_2$ in V_2 is $\left\langle |\mathbf{E}_{\text{inc},1}(\mathbf{x}_2)|^2 \right\rangle = 4\varepsilon_0 \omega \Theta (\text{Im}\,\chi) \int_{V_1} \|\mathbf{G}_1(\mathbf{x}_2, \mathbf{x}_1)\|_F^2$, where $\|\cdot\|_F$ denotes the Frobenius norm [49]. By reciprocity [50] one can exchange the positions in the integrand,

$\mathbf{x}_1 \leftrightarrow \mathbf{x}_2$ (while transposing the GF, but the transpose does not affect the norm), such that emission from V_1 is equivalent to *absorption* for free-space sources in V_2, as in Fig. 1(c). Absorption is bounded by energy conservation [42], limiting the emitted-field magnitude:

$$\left\langle |\mathbf{E}_{\text{inc},1}(\mathbf{x}_2)|^2 \right\rangle \leq 4\varepsilon_0 \omega \Theta \frac{|\chi_1|^2}{\text{Im}\,\chi_1} \int_{V_1} \|\mathbf{G}_0(\mathbf{x}_1, \mathbf{x}_2)\|_F^2 \quad (3)$$

where $\mathbf{G}_0$ is the *free-space* GF, cf. Fig. 1(d). Inserting Eq. (3) into Eq. (2) and separating the Planck spectrum by Eq. (1), the maximum flux between two bodies is

$$\Phi(\omega) \leq \frac{2}{\pi} \frac{|\chi_1(\omega)|^2}{\text{Im}\,\chi_1(\omega)} \frac{|\chi_2(\omega)|^2}{\text{Im}\,\chi_2(\omega)} \int_{V_1} \int_{V_2} \|\mathbf{G}_0(\mathbf{x}_1, \mathbf{x}_2)\|_F^2. \quad (4)$$

The limit of Eq. (4) can be further simplified. In the near field, $\mathbf{G}_0$ is ideally dominated by the quasistatic term $\sim 1/r^3$, which is primarily responsible for the evanescent waves that enable greater-than-black-body heat-transfer rates [4, 7]. Dropping higher-order terms (further discussed in [51]), we bound Eq. (4) by integrating over the infinite half-spaces containing V_1 and V_2, assuming a separating plane between the two bodies. (If not, e.g. between two curved surfaces, only the coefficients change.) For bodies separated by a distance d, the integral over the (infinite) area A is given by [51] $\int_{V_1,V_2} \|\mathbf{G}_0\|_F^2 = A/32\pi d^2$, yielding flux limits per area or relative to a black body with flux $\Phi_{\text{BB}} = k^2 A/4\pi^2$ [4]:

$$\frac{\Phi(\omega)}{A} \leq \frac{1}{16\pi^2 d^2} \frac{|\chi_1(\omega)|^2}{\text{Im}\,\chi_1(\omega)} \frac{|\chi_2(\omega)|^2}{\text{Im}\,\chi_2(\omega)}. \quad (5)$$

$$\frac{\Phi(\omega)}{\Phi_{\text{BB}}(\omega)} \leq \frac{1}{4(kd)^2} \frac{|\chi_1(\omega)|^2}{\text{Im}\,\chi_1(\omega)} \frac{|\chi_2(\omega)|^2}{\text{Im}\,\chi_2(\omega)}. \quad (6)$$

Eqs. (4–6) are fundamental limits to the near-field spectral heat flux between two bodies and form the central results of this Letter. They arise from basic limitations to the currents that can be excited in dissipative media, and their derivations further suggest physical characteristics of the optimal response in near-field heat transfer: an *optimal emitter*

enhances and absorbs near-field waves from reciprocal external sources *in the absence of the absorber* whereas an optimal absorber enhances and absorbs near-field waves from the emitter, *in the presence of the emitter*. These principles can be understood by working backwards through Fig. 1. The optimal-emitter condition identifies the largest field that can be generated in an exterior volume (V_2) by considering the reciprocal absorption problem, per Fig. 1(c). Reinserting the absorber, cf. Fig. 1(b), should not reflect the emitted field but rather enhance and absorb it. Because heat flux is symmetric with respect to absorber–emitter exchange, both bodies should satisfy each condition (induced currents proportional to source fields). Eq. (4) can be interpreted as sources throughout the emitter generating free-space dipolar fields $\boldsymbol{G}^0$ enhanced by $|\chi_1|^2 / \operatorname{Im}\chi_1$, which are further enhanced by $|\chi_2|^2 / \operatorname{Im}\chi_2$ and absorbed. The dipole–dipole interactions are bounded by their separation distance [43, 52], leading to simple shape-independent limits in Eqs. (4–6). Ideal structures that achieve these limits can have significantly greater heat transfer than black bodies, even if their spectral flux has a narrow bandwidth. Whereas the heat transfer between black bodies in the far field is $H/A = \sigma_{\mathrm{SB}}T^4$, where σ_{SB} is the Stefan–Boltzmann constant [36], a straightforward calculation citeNote1 shows that ideal near-field heat exchange over a narrow bandwidth $\Delta\omega/\omega = \operatorname{Im}\chi/|\chi|$, typical of plasmonic systems [53, 54], can achieve per-area transfer rates of

$$\frac{H}{A} \approx \sigma_{\mathrm{SB}}T^4 \frac{2}{7(kd)^2} \frac{|\chi|^3}{\operatorname{Im}\chi}, \tag{7}$$

exhibiting both distance and material enhancements relative to the Stefan–Boltzmann rate.

The limits generalize [51] to local media with tensor susceptibilities via the replacement $|\chi|^2/\operatorname{Im}\chi \to \left\| \boldsymbol{\chi}(\operatorname{Im}\boldsymbol{\chi})^{-1}\boldsymbol{\chi}^\dagger \right\|_2$. Nonlocal effects, which appear below 10nm length scales [55] and which regularize the $1/d^2$ divergence [4], are outside the scope of these limits, but we believe that a generalization to nonlocal $\boldsymbol{\chi}$ is possible and have preliminary results [56] suggesting that "hydrodynamic" [57, 58] nonlocal materials cannot not surpass the local-$\boldsymbol{\chi}$ bounds.

Dipolar Interactions—If one of the bodies is small enough for its response to be dipolar, the optimal-absorber and optimal-emitter conditions converge: the polarization currents induced in each structure by free-space dipoles in place of the opposite structure must be proportional to the incident fields. This condition is satisfied for two-dipole transfer, and the enhancement of the emitted and absorbed fields is possible via "plasmonic" resonances in metallic nanoparticles. For two identical particles with volumes V, tip-to-center-of-mass distances r, and tip-to-tip separation d, Eq. (4) limits the flux:

$$[\Phi(\omega)]_{\mathrm{dipole–dipole}} \leq \frac{3}{4\pi^3} \frac{|\chi_1(\omega)|^2}{\operatorname{Im}\chi_1(\omega)} \frac{|\chi_2(\omega)|^2}{\operatorname{Im}\chi_2(\omega)} \frac{V^2}{(2r+d)^6}. \tag{8}$$

The radiative flux between quasistatic metal spheres is known analytically [4] and peaks at the limit given by Eq. (8).
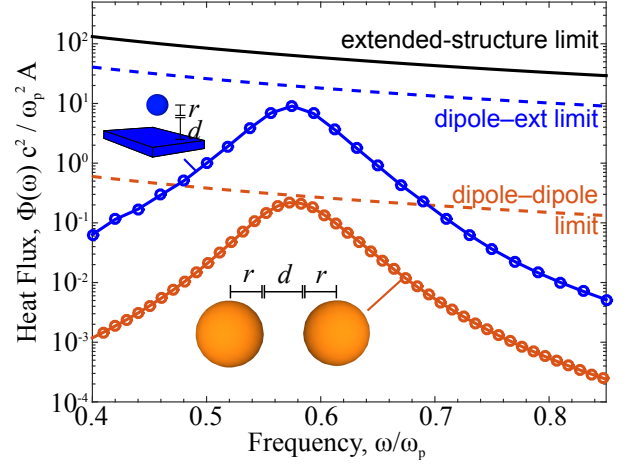

FIG. 2. Comparison of heat flux in sphere–sphere and sphere–plate structures to the analytical limits of Eqs. (8,9). Two Drude metal spheres (orange circles, fit to a solid line) approach the dipole–dipole limit (dashed orange) at their resonant frequency, $\omega_{\mathrm{res}} \approx \omega_p/\sqrt{3}$. A sphere and a plate (blue circles) approach within a factor of two of the limit between dipolar and extended objects (dashed blue), if the material resonance of the plate is slightly modified (see text). In each case the separation is $d = 0.1c/\omega_{\mathrm{res}}$, with sphere radii $r = d/5$. The flux rates exhibit the material enhancement factor $|\chi|^4/(\operatorname{Im}\chi)^2$, but not the near-field enhancement factor, due to the lack of large-area interactions. The sphere area A is taken to be the cross-section πr^2.

Heat transfer between a dipole and an extended structure is limited by integrating over the half-space occupied by any extended structure, yielding a maximum flux

$$[\Phi(\omega)]_{\mathrm{dipole\text{-}to\text{-}ext}} \leq \frac{1}{8\pi^2} \frac{|\chi_1(\omega)|^2}{\operatorname{Im}\chi_1(\omega)} \frac{|\chi_2(\omega)|^2}{\operatorname{Im}\chi_2(\omega)} \frac{V}{(r+d)^3}, \tag{9}$$

where $r+d$ is the distance between the extended structure and the particle's center. Heat flux between a sphere and a bulk metal, each supporting a plasmonic mode, can achieve half of the maximum flux [4, 51, 59] if the resonances align. This geometry falls short by a factor of two because planar surface plasmons exist only for TM polarization [60], and thus the planar structure reflects near-field TE-polarized light emitted by the sphere. Neither structure exhibits the $1/d^2$ enhancement factor, which for dipolar coupling ($\sim 1/d^6$) requires interactions over two extended areas.

Fig. 2 compares flux rates for sphere–sphere (orange circles) and sphere–plate (blue circles) geometries, computed by the fluctuating-surface current method [61–63], to the limits of Eqs. (8,9) (orange and blue dashed lines, resp.). The spheres are modeled by Drude susceptibilities [44] with plasma frequency ω_p and loss rate $\gamma = 0.1\omega_p$. The "plate" is simulated by a very large ellipsoid (volume $\approx 7000\times$ larger than the sphere) comprising a material with a modified plasma frequency, $\omega_{p,\mathrm{pl}} = \sqrt{2/3}\omega_p$, and a modified loss rate, $\gamma_{\mathrm{pl}} = 2\gamma/3$, to align the resonant frequencies of the sphere and plate without modifying the flux limit. In each case the separation distance $d = 0.1c/\omega_{\mathrm{res}}$ and the sphere radii are $r = d/5$.
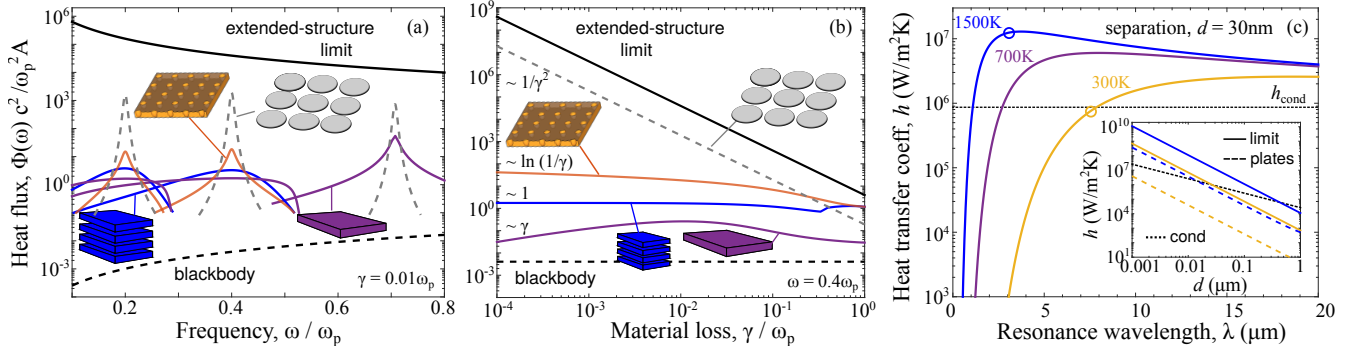
FIG. 3. (a,b) Comparison of heat flux between mirror images of large-area Drude-metal structures separated by $d = 0.1c/\omega_p$. (a) Structures optimized for maximum flux at three frequencies, $\omega = (0.2, 0.4, 1/\sqrt{2})\omega_p$, for a material loss rate $\gamma = 0.01\omega_p$. Thin films (purple), hyperbolic metamaterials (blue), and elliptical metamaterials (orange) exceed black-body enhancements but fall far short of the limit (black) from Eq. (5). The dashed silver line represents the heat transfer for an idealized plasmonic-particle array without multiple scattering. (b) Optimized structures as a function of loss rate, for $\omega = 0.4\omega_p$. Each structure exhibits the $1/d^2$ near-field enhancement factor, but only the idealized particle array exhibits the $|\chi|^4/(\text{Im}\,\chi)^2 \sim 1/\gamma^2$ material enhancement factor. (c) Frequency-integrated heat transfer coefficient of a structure that reaches the single-frequency limit in Eq. (5) over a narrow bandwidth $\Delta\omega \propto \gamma$. Radiative heat exchange in this limit shows the possibility of surpassing conductive heat transfer through air (dotted) at $T = 300$K (gold), which is not possible for plate–plate configurations (inset, dashed), and of significant further enhancements at higher temperatures (blue, purple).

The computations support the analytical result that the dipolar limits can be approached to within at least a factor of two.

Extended Structures—For extended structures that do not behave like single dipoles, the optimal-absorber constraint is more demanding in that the absorber should enhance the emitted field while accounting for interactions between the two bodies. We will show that common planar structures do not exhibit this behavior but that nanostructured media offer the possibility of approaching it.

Bulk metals (negative-permittivity materials) support surface plasmons that enable greater-than-blackbody heat flux at their resonant frequency. Individually, a single metal interface nearly satisfies the optimal-emitter condition, emitting near-field waves over a broad bandwidth of surface-parallel wavevectors (which enabled the nearly optimal sphere–plate transfer above). However, when a second metal is brought close to the first, it *reflects* most of the incident field, except over a narrow wavevector-bandwidth, due to multiple-scattering effects between the bodies. The failure of the two-metal geometry to achieve the optimal-absorber condition leads to a peak spectral heat flux, at the surface-plasmon frequency ω_{sp}, of approximately citeNote1

$$\left[\frac{\Phi(\omega_{\text{sp}})}{A}\right]_{\text{plate-to-plate}} = \frac{1}{4\pi^2 d^2} \ln\left[\frac{|\chi|^4}{4(\text{Im}\,\chi)^2}\right] \qquad (10)$$

which is significantly smaller than the limit in Eq. (5) due to the weak, logarithmic material enhancement. Eq. (10) appears to be new and is a significantly better approximation than planar bounds that do not account for material loss [10, 16], as discussed in the SM citeNote1. The shortcomings of the bulk-metal interactions cannot be overcome with simple metamaterial or thin-film geometries. The flux rate between hyperbolic metamaterials (HMMs) is material-independent [21, 51]. Optimal thin films behave similarly to HMMs [31], thereby also

falling short of the limits. "Elliptical" metamaterials, with nearly isotropic effective permittivities, exhibit resonances for $\chi_{\text{eff}} \approx -2$ and thus transfer heat at a rate similar to Eq. (10), limited by the same interference effects discussed above, and because $|\chi_{\text{eff}}|^4 \ll |\chi|^4$.

Fig. 3(a,b) demonstrates the shortcomings of such structures, showing the computed heat flux between mirror images of thin-film (purple), hyperbolic-metamaterial (blue), and elliptical-metamaterial (orange) structures, as a function of (a) frequency and (b) material-loss rate, for a fixed separation $d = 0.1c/\omega_p$. Assuming smooth surfaces without roughness, the structural parameters are computationally optimized citeNote1 using a derivative-free local optimization algorithm [64, 65]. Fig. 3(b) shows that the sub-optimal performance can be attributed primarily to the fact that the structures do not exhibit the material enhancement factor $|\chi|^4/(\text{Im}\,\chi)^2 \sim 1/\gamma^2$, as predicted by Eq. (10) and due to the significant reflections in such geometries.

The spectral heat flux of the limit in Eq. (4) can be interpreted as the exchange of enhanced free-space dipole fields, as discussed above. Guided by this intuition, we include in Fig. 3(a,b) the heat flux between close-packed arrays of oblate disk ellipsoids (dashed silver lines), small enough to be dipolar. We idealize their response as the additive sum of Eq. (8) over a lattice neglecting multiple scattering (i.e. in a Born approximation) [66] and accounting for the polarization-dependence of non-spherical ellipsoids [37]. This structure combines the individual-particle interactions that exhibit the material enhancement (which planar bodies do not) with the large-area interactions that exhibit $1/d^2$ near-field enhancement (which isolated bodies do not). Fig. 3(a,b) suggest the possibility for two to three orders of magnitude enhancement by periodic structuring and tailored local interactions.

Experimental measurements of radiative heat transfer are

done in vacuum [6, 12, 13] because radiative transfer is dominated by conductive transfer through an air gap. Achieving the limits presented here, even over a narrow bandwidth, could transform this landscape. Fig. 3(c) shows the heat-transfer coefficient $h = \int \Phi(\partial\Theta/\partial T)\mathrm{d}\omega$ for extended Drude-metal structure with loss rates $\gamma = 0.01\omega_p$ (appropriate e.g. for Ag and Au [67]). For Lorentzian-shaped energy transfer with tunable center frequency $\omega_{\mathrm{res}} = \omega_p/\sqrt{2}$, peaked at the limit given by Eq. (5), with a bandwidth $\Delta\omega = \gamma$ [51, 53, 54], radiative transfer can surpass conductive (thermal conductivity $\kappa_{\mathrm{air}} = 0.026\mathrm{W/m\cdot K}$ [68]) even at $T = 300\mathrm{K}$. In the inset we fix the wavelengths at $\lambda = 7.6\mu m$ for $T = 300\mathrm{K}$ and $\lambda = 3\mu m$ for $T = 1500K$, and plot h as a function of distance for plate–plate (dashed) and optimal (solid) transfer. We find that radiative transfer can surpass conductive at separation of $d = 50\mathrm{nm}$ at 300K and almost $d = 0.5\mu m$ at $T = 1500\mathrm{K}$, gap sizes that are readily achievable in experiments.

Radiative heat transfer at the nanoscale is a nascent but growing field. Calculations have primarily been for dipolar [5, 10, 59] or highly symmetric bodies [8–14, 18–23, 25–31, 69–71], with computational study of more complex geometries possible only recently [35, 62, 63, 72–74]. We have show that, guided by the physical principles presented here, a targeted search through the mostly uncharted near-field design space offers the prospect of orders-of-magnitude enhancements in radiative energy transfer.

[1] D. Polder and M. Van Hove, Physical Review B **4**, 3303 (1971).
[2] S. M. Rytov, Y. A. Kravtsov, and V. I. Tatarskii, *Principles of statistical radiophysics* (Springer-Verlag New York Inc., New York, NY, 1988).
[3] J.-P. Mulet, K. Joulain, R. Carminati, and J.-J. Greffet, Microscale Thermophysical Engineering **6**, 209 (2002).
[4] K. Joulain, J.-P. Mulet, F. Marquier, R. Carminati, and J.-J. Greffet, Surface Science Reports **57**, 59 (2005).
[5] A. I. Volokitin and B. N. J. Persson, Reviews of Modern Physics **79**, 1291 (2007).
[6] E. Rousseau, A. Siria, G. Jourdan, S. Volz, F. Comin, J. Chevrier, and J.-J. Greffet, Nature Photonics **3**, 514 (2009).
[7] S. Basu, Z. M. Zhang, and C. J. Fu, International Journal of Energy Research **33**, 1203 (2009).
[8] J. J. Loomis and H. J. Maris, Physical Review B **50**, 18517 (1994).
[9] J. B. Xu, K. Läuger, R. Möller, K. Dransfeld, and I. H. Wilson, Journal of Applied Physics **76**, 7209 (1994).
[10] J. B. Pendry, Journal of Physics: Condensed Matter **11**, 6621 (1999).
[11] C. Fu and Z. Zhang, International Journal of Heat and Mass Transfer **49**, 1703 (2006).
[12] L. Hu, A. Narayanaswamy, X. Chen, and G. Chen, Applied Physics Letters **92**, 133106 (2008).
[13] R. S. Ottens, V. Quetschke, S. Wise, A. A. Alemi, R. Lundock, G. Mueller, D. H. Reitze, D. B. Tanner, and B. F. Whiting, Physical Review Letters **107**, 014301 (2011), arXiv:1103.2389.
[14] P. J. Van Zwol, K. Joulain, P. Ben-Abdallah, and J. Chevrier, Physical Review B **84**, 161413 (2011).
[15] S. Basu and Z. M. Zhang, Journal of Applied Physics **105**, 093535 (2009).
[16] P. Ben-Abdallah and K. Joulain, Physical Review B **82**, 121419 (2010), arXiv:1009.4598.
[17] E. Nefzaoui, Y. Ezzahri, J. Drévillon, and K. Joulain, The European Physical Journal Applied Physics **63**, 30902 (2013), arXiv:1302.1718.
[18] S.-A. Biehs, P. Ben-Abdallah, F. S. S. Rosa, K. Joulain, and J.-J. Greffet, Optics Express **19**, A1088 (2011).
[19] M. Francoeur, S. Basu, and S. J. Petersen, Optics Express **19**, 18774 (2011).
[20] K. Joulain, J. Drevillon, and P. Ben-Abdallah, Physical Review B **81**, 165119 (2010).
[21] S.-A. Biehs, M. Tschikin, and P. Ben-Abdallah, Physical Review Letters **109**, 104301 (2012).
[22] S.-A. Biehs, M. Tschikin, R. Messina, and P. Ben-Abdallah, Applied Physics Letters **102**, 131106 (2013).
[23] Y. Guo and Z. Jacob, Optics Express **21**, 15014 (2013).
[24] E. E. Narimanov and I. I. Smolyaninov, in *Quantum Electronics and Laser Science Conference* (Optical Society of America, 2012).
[25] S.-A. Biehs, D. Reddig, and M. Holthaus, The European Physical Journal B **55**, 237 (2007).
[26] M. Francoeur, M. P. Menguc, and R. Vaillon, Applied Physics Letters **93**, 043109 (2008).
[27] M. Francoeur, M. Pinar Mengüç, and R. Vaillon, Journal of Quantitative Spectroscopy and Radiative Transfer **110**, 2002 (2009).
[28] P. Ben-Abdallah, K. Joulain, J. Drevillon, and G. Domingues, Journal of Applied Physics **106**, 044306 (2009).
[29] M. Francoeur, M. P. Mengüç, and R. Vaillon, Journal of Physics D: Applied Physics **43**, 075501 (2010).
[30] S. Basu and M. Francoeur, Applied Physics Letters **98**, 243120 (2011).
[31] O. D. Miller, S. G. Johnson, and A. W. Rodriguez, Physical Review Letters **112**, 157402 (2014), arXiv:1311.5812.
[32] M. D. Whale and E. G. Cravalho, IEEE Transactions on Energy Conversion **17**, 130 (2002).
[33] M. Laroche, R. Carminati, and J.-J. Greffet, Journal of Applied Physics **100**, 063704 (2006).
[34] P. Bermel, M. Ghebrebrhan, W. Chan, Y. X. Yeng, M. Araghchini, R. Hamam, C. H. Marton, K. F. Jensen, M. Soljačić, J. D. Joannopoulos, S. G. Johnson, and I. Celanovic, Optics Express **18**, A314 (2010).
[35] A. W. Rodriguez, O. Ilic, P. Bermel, I. Celanovic, J. D. Joannopoulos, M. Soljačić, and S. G. Johnson, Physical Review Letters **107**, 114302 (2011).
[36] J. H. Lienhard IV and J. H. Lienhard V, *A Heat Transfer Textbook*, 4th ed. (Dover, 2011).
[37] C. F. Bohren and D. R. Huffman, *Absorption and Scattering of Light by Small Particles* (John Wiley & Sons, New York, NY, 1983).
[38] S. G. Johnson, P. Bienstman, M. A. Skorobogatiy, M. Ibanescu, E. Lidorikis, and J. D. Joannopoulos, Physical Review E **66**,

066608 (2002).

[39] D.-H. Kwon and D. M. Pozar, IEEE Transactions on Antennas and Propagation **57**, 3720 (2009).

[40] I. Liberal, Y. Ra'di, R. Gonzalo, I. Ederra, S. A. Tretyakov, and R. W. Ziolkowski, IEEE Transactions on Antennas and Propagation **62**, 4726 (2014), arXiv:1402.4726.

[41] J.-P. Hugonin, M. Besbes, and P. Ben-Abdallah, Physical Review B **91**, 180202 (2015), arXiv:1502.02409.

[42] O. D. Miller, A. G. Polimeridis, M. T. H. Reid, C. W. Hsu, B. G. DeLacy, J. D. Joannopoulos, M. Soljačić, and S. G. Johnson, Submitted, arXiv: 1503.03781 (2015).

[43] D. A. B. Miller, Applied Optics **39**, 1681 (2000).

[44] J. D. Jackson, *Classical Electrodynamics, 3rd Ed.* (John Wiley & Sons, Inc., 1999).

[45] R. G. Newton, American Journal of Physics **44**, 639 (1976).

[46] D. R. Lytle, P. S. Carney, J. C. Schotland, and E. Wolf, Physical Review E **71**, 056610 (2005).

[47] H. Hashemi, C.-W. Qiu, A. P. McCauley, J. D. Joannopoulos, and S. G. Johnson, Physical Review A **86**, 013804 (2012).

[48] W. C. Chew, *Waves and fields in inhomogeneous media*, Vol. 522 (IEEE press New York, 1995).

[49] L. N. Trefethen and D. Bau, *Numerical Linear Algebra* (Society for Industrial and Applied Mathematics, Philadelphia, PA, 1997).

[50] E. J. Rothwell and M. J. Cloud, *Electromagnetics* (CRC Press LLC, 2001).

[51] See Supplementary Material [url], which includes Refs. 75 and 76.

[52] R. Piestun and D. A. B. Miller, Journal of the Optical Society of America A **17**, 892 (2000).

[53] F. Wang and Y. R. Shen, Physical Review Letters **97**, 206806 (2006).

[54] A. Raman, W. Shin, and S. Fan, Physical Review Letters **110**, 183901 (2013).

[55] F. Singer, Y. Ezzahri, and K. Joulain, Journal of Quantitative Spectroscopy and Radiative Transfer **154**, 55 (2015).

[56] O. D. Miller et al., in progress.

[57] C. Ciracì, R. T. Hill, J. J. Mock, Y. Urzhumov, A. I. Fernández-Domínguez, S. A. Maier, J. B. Pendry, A. Chilkoti, and D. R. Smith, Science (New York, N.Y.) **337**, 1072 (2012).

[58] S. Raza, S. I. Bozhevolnyi, M. Wubs, and N. Asger Mortensen, Journal of Physics: Condensed Matter **27**, 183204 (2015).

[59] J. P. Mulet, K. Joulain, R. Carminati, and J. J. Greffet, Applied Physics Letters **78**, 2931 (2001).

[60] S. A. Maier, *Plasmonics: Fundamentals and Applications* (Springer Science & Business Media, 2007).

[61] M. T. H. Reid, http://homerreid.com/scuff-EM .

[62] A. W. Rodriguez, M. T. H. Reid, and S. G. Johnson, Physical Review B **86**, 220302 (2012), arXiv:1206.1772.

[63] A. W. Rodriguez, M. T. H. Reid, and S. G. Johnson, Physical Review B **88**, 054305 (2013).

[64] M. J. D. Powell, in *Advances in Optimization and Numerical Analysis* (Springer, 1994) pp. 51–67.

[65] S. G. Johnson, http://ab-initio.mit.edu/nlopt .

[66] A. D. Phan, T.-L. Phan, and L. M. Woods, Journal of Applied Physics **114**, 214306 (2013).

[67] E. D. Palik, *Handbook of Optical Constants of Solids*, edited by E. D. Palik (Elsevier Science, 1998).

[68] W. M. Haynes, *CRC handbook of chemistry and physics* (CRC press, 2013).

[69] C. Otey and S. Fan, Physical Review B **84**, 245431 (2011), arXiv:1103.2668.

[70] A. Perez-Madrid, L. C. Lapas, and J. M. Rubi, PLOS ONE **8**, e58770 (2013).

[71] Y. Zheng and A. Ghanekar, Journal of Applied Physics **117**, 064314 (2015).

[72] A. P. McCauley, M. T. H. Reid, M. Krüger, and S. G. Johnson, Physical Review B **85**, 165104 (2012).

[73] A. Pérez-Madrid, J. M. Rubí, and L. C. Lapas, Physical Review B **77**, 155417 (2008), arXiv:0801.1768.

[74] C. R. Otey, L. Zhu, S. Sandhu, and S. Fan, Journal of Quantitative Spectroscopy and Radiative Transfer **132**, 3 (2014).

[75] M. Cardona, American Journal of Physics **39**, 1277 (1971).

[76] J. A. Kong, *Theory of electromagnetic waves*, Vol. 1 (Wiley-Interscience, New York, NY, 1975).